Strong-Field Resonant Dynamics in Semiconductors

Michael S. Wismer, Stanislav Yu. Kruchinin, Marcelo Ciappina, Mark I. Stockman, and Vladislav S. Yakovlev

Phys. Rev. Lett. **116**, 197401 — Published 10 May 2016

DOI: 10.1103/PhysRevLett.116.197401

Strong-Field Resonant Dynamics in Semiconductors

Michael S. Wismer,[1,*] Stanislav Yu. Kruchinin,[1,†] Marcelo Ciappina,[1] Mark I. Stockman,[2,‡] and Vladislav S. Yakovlev[1,2,§]

[1] *Max-Planck-Institut für Quantenoptik, Hans-Kopfermann-Str. 1, 85748 Garching, Germany*
[2] *Center for Nano-Optics (CeNO) and Department of Physics and Astronomy, Georgia State University, Atlanta, Georgia 30340, USA*

(Dated: March 1, 2016)

We predict that a direct bandgap semiconductor (GaAs) resonantly excited by a strong ultrashort laser pulse exhibits a novel regime: kicked anharmonic Rabi oscillations (KARO). In this regime, Rabi oscillations are strongly coupled to intraband motion, and interband transitions mainly take place when electrons pass near the Brillouin zone center where electron populations undergo very rapid changes. Asymmetry of the residual population distribution induces an electric current controlled by the carrier-envelope phase of the driving pulse. The predicted effects are experimentally observable using photoemission and terahertz spectroscopies.

Effect of strong electric fields on crystalline solids was long considered important as introduced by Zener [1] and developed by Keldysh [2]. Recently, a novel field studying interaction of few-cycle high-intensity (with fields reaching or exceeding internal fields in the matter) optical pulses with solids has attracted a great deal of attention [3–12]. One of the most significant directions of the recent research was strong-field interaction of ultrashort pulses with transparent solids where carrier frequency ω_0 and pulse bandwidth $\Delta\omega$ were well within the bandgap: $\hbar\omega_0, \hbar\Delta\omega \ll E_g$, that is, the interaction was nonresonant. In this case, the characteristic response time τ is determined by the band gap: $\tau \gtrsim \hbar/E_g$ [6]. Consequently, light-induced processes are subcycle and depend on the carrier-envelope phase (CEP) [13].

Resonant ($\hbar\omega_0 \sim E_g$) interaction of intense ultrashort pulses with absorbing solids was also investigated. The CEP controllability of electron dynamics in this regime was mostly studied in the context of carrier-wave Rabi flopping (CWRF) [14–17], where the motion of charge carriers within bands was neglected. Also perturbative $\omega+2\omega$ interference was investigated [18, 19]. In this case, a relatively weak field limits the scope of the intraband motion.

Thus, in previously studied regimes, either intraband electron dynamics were important, or resonant light absorption played a dominant role. Here we consider a new strong-field regime where intraband dynamics fundamentally affect the resonant excitation. In this regime, transitions between bands occur within a small fraction of an optical cycle. Their quantum interference is predicted to cause a strong residual ballistic electric current that is controllable by the CEP.

We solve the length-gauge optical Bloch equations with intraband displacement terms [8, 20]:

$$\frac{\partial}{\partial t}\rho_{ij} = \left[\frac{\delta_{ij}-1}{T_2} + \frac{i}{\hbar}(E_i - E_j)\right]\rho_{ij} + \frac{1}{\hbar}\boldsymbol{F}(t)\big(e\nabla_{\boldsymbol{k}}\rho_{ij} - i[\hat{\boldsymbol{d}},\hat{\rho}]_{ij}\big). \quad (1)$$

Here, $\rho(\boldsymbol{k},t)$ is a density matrix, its diagonal elements, $n_i(\boldsymbol{k},t) = \rho_{ii}(\boldsymbol{k},t)$, are dimensionless probabilities to find an electron with crystal momentum $\boldsymbol{k}$ in band i, T_2 is dephasing time introduced phenomenologically, $e>0$ is the elementary charge, and $\boldsymbol{d}_{ij}(\boldsymbol{k}) = e\langle\psi_i(\boldsymbol{k})|i\nabla_{\boldsymbol{k}}|\psi_j(\boldsymbol{k})\rangle$ are dipole matrix elements that form matrix $\hat{\boldsymbol{d}}$. We obtained $\boldsymbol{d}_{ij}(\boldsymbol{k})$ and the band energies $E_i(\boldsymbol{k})$ using the Wien2K code [21]. We assume that the electric field of the laser pulse *in the medium* $\boldsymbol{F}(t)$ is linearly polarized along the $\Gamma-\mathrm{X}$ direction in the Brillouin zone of GaAs, where the X point is at $k_{\max} = 1.11\,\text{Å}^{-1}$. This choice eliminates second-order nonlinear effects, in particular, optical rectification [22]. We will denote the field projection on the $\Gamma-\mathrm{X}$ direction as $F(t)$ and its amplitude as F_0. The specific form of $F(t)$ is described in Supplemental Material [23]. This is a 5-fs pulse with a central (carrier) photon energy of $\hbar\omega_0 = E_g = 1.55$ eV.

Let us make a few estimates. Nondestructive measurements on GaAs with few-cycle pulses were reported for $F_0 = 0.4$ V/Å (a peak intensity of 2×10^{12} W/cm^2), where the onset of CWRF was observed [15, 17]. This field is much smaller than that required to accelerate an electron from the Γ point ($\boldsymbol{k}=0$) to the boundary of the Brillouin zone, which is $F_0 = 0.9$ V/Å for $\hbar\omega_0 = 1.55$ eV. Using $d = 5\ e\cdot$Å [15] for transitions between the light-hole valence band (VB) and the lowest conduction band (CB), we estimate the ratio of the Rabi frequency $\Omega_R = dF_0/\hbar$ to the laser frequency as $\Omega_R/\omega_0 \approx F_0/(0.3\text{ V/Å})$. We also note that our laser pulse is much shorter than the momentum relaxation time in GaAs, which is ~ 200 fs [24, 25].

Figure 1 shows the residual current density,

$$j\left(F_0,\varphi_{\mathrm{CE}}\right) = -\frac{2e}{(2\pi)^3}\sum_i \int_{\mathrm{BZ}} d^3k\, n_i(\boldsymbol{k},t_{\max})\hat{\boldsymbol{e}}\boldsymbol{v}_i(\boldsymbol{k}), \quad (2)$$

for the cases of two [Figs. 1(a)-(c)] and six [Figs. 1(d)-(f)] bands, as well as for different values of T_2. Using more than three conduction bands does not qualitatively change our results [23]. In Eq. (2), $\boldsymbol{v}_i(\boldsymbol{k}) = \hbar^{-1}\nabla_{\boldsymbol{k}}E_i$ is

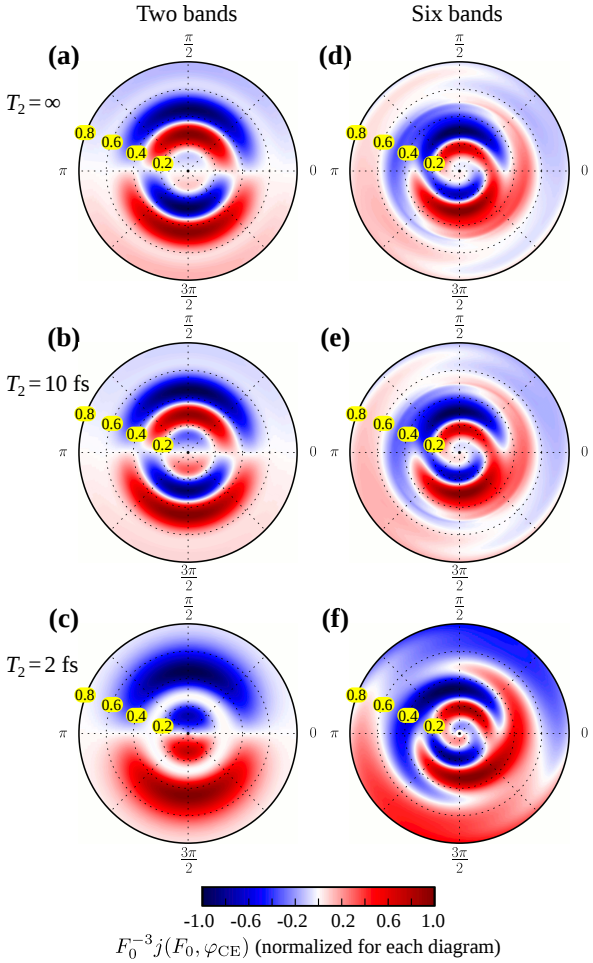

FIG. 1. (Color online) The residual current density $j(F_0, \varphi_{CE})$. In these diagrams, the distance to the origin corresponds to the pulse amplitude F_0, which varies from zero to 0.8 V/Å, while the angle to the horizontal axis encodes the carrier-envelope phase φ_{CE}. The color coding of $F_0^{-3} j(F_0, \varphi_{CE})$ is individually normalized for each diagram. Panels (a)–(c) show two-band results (1 VB, 1 CB), while panels (d)–(f) display outcomes of six-band (3 VBs, 3 CBs) calculations. Each horizontal pair of plots corresponds to a certain value of dephasing time T_2 as indicated by the labels.

group velocity in band i, and $t_{max} = 36.2$ fs is the final time of our simulations. When the field is weak, the photocurrent is excited due to the $\omega+2\omega$ interference [18, 19]. In this case, it is known that $j_{max}(F_0) \propto F_0^3$—cf. Fig. 2. This is due to the fact that the probability amplitudes of one- and two-photon processes are proportional to F_0 and F_0^2, respectively, while their interference makes a contribution proportional to F_0^3. In Fig. 2, this cubic dependence breaks down for $F_0 \gtrsim 0.1$ V/Å, which we visualize in Fig. 1 by representing $F_0^{-3} j(F_0, \varphi_{CE})$ with color coding. In Fig. 1, the results obtained for two and six bands differ significantly, which is consistent with recent findings [11]. However, they also share a few remarkable features.

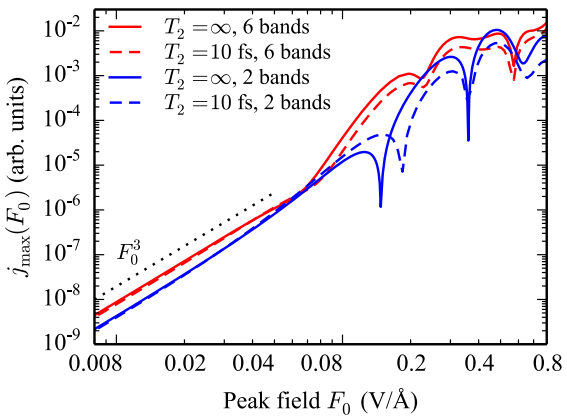

FIG. 2. (Color online) The maximal value of the residual current density $j_{max}(F_0) = \max_{\varphi_{CE}}[j(F_0, \varphi_{CE})]$. The solid and dashed lines were obtained with $T_2 = \infty$ and $T_2 = 10$ fs, respectively. Red curves represent six-band calculations (3 VBs, 3 CBs), whereas blue curves show the two-band results (1 VB, 1 CB).

First, we observe CEP-controlled light-induced residual current, which implies that it is due to ultrafast, subcycle processes. The cases of no polarization relaxation ($T_2 = \infty$) [panels (a) and (d)] and fast dephasing [$T_2 = 10$ fs, panels (b) and (e)] differ very little, which suggests that there is fast effective dephasing within the purely Hamiltonian system described by the Schrödinger equation. Note that the fastest electron dephasing time in semiconductors (GaAs) was measured to be $T_2 \sim 14$ fs [26], which was consistent with theory [27]. At the same time, recent experiments on high-harmonic generation in solids [8–12] suggest that dephasing times in the strong-field regime may be on the order of femtoseconds, so we also present results for $T_2 = 2$ fs. We note that T_2 has a stronger impact on the two-band results.

Second, for any chosen CEP, $j(F_0, \varphi_{CE})$ changes its sign at certain values of F_0. In the two-band model, the maximum magnitude of the current at any field amplitude is always obtained for the antisymmertic pulse ($\varphi_{CE} = \pm\pi/2$). In contrast, for more realistic six-band calculations, the maximum current non-trivially depends on the CEP, which causes the appearance of "vortices" in panels (d)–(f).

Third, starting from $F_0 \sim 0.2$ V/Å, the residual current is much stronger than that obtained by extrapolating the weak-field current according to the $\propto F_0^3$ law. This fact is more clearly seen in Fig. 2, from which we also conclude that dephasing tends to reduce the magnitude of the residual current.

To gain more insight, we analyze in Fig. 3 the residual population $n_{c_1}(k, t_{max})$ of the lowest conduction band (c_1). Higher bands contribute significantly less to the electric current. As we have already pointed out, dephasing with a typical rate of $T_2 \gtrsim 10$ fs has a minor effect;

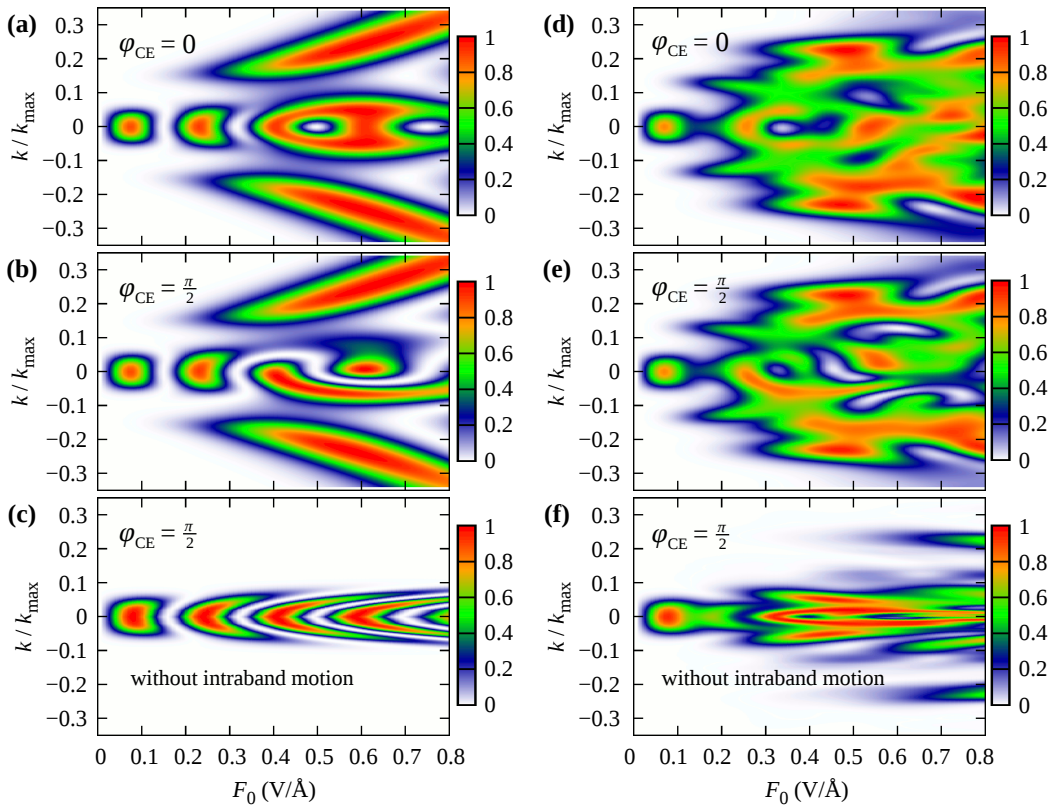

FIG. 3. (Color online) The residual population of the lowest conduction band $n_{c_1}(k, t_{max})$ in simulations with two (a)–(c) and six (d)–(f) bands without dephasing ($T_2 = \infty$). The CEP of the laser pulse is $\varphi_{CE} = 0$ in panels (a), (d) and $\pi/2$ in the other plots. Panels (c), (f) display population distributions obtained without intraband motion.

therefore we set $T_2 = \infty$. We start with the case of two bands displayed in Figs. 3(a)–(c) where it is easier to disentangle different processes. For $\varphi_{CE} = 0$ [panel (a)], the k-resolved population is symmetric, so that the residual intraband current is close to zero, in accord with Fig. 1. For $\varphi_{CE} = \pi/2$ [panel (b)], the residual conduction-band population becomes highly asymmetric in $\pm k$ in the region $F_0 \gtrsim 0.3$ V/Å and $|k|/k_{max} \lesssim 0.1$. As Fig. 3(c) demonstrates, intraband motion plays a key role here. Eliminating it by dropping the term $\propto \boldsymbol{F}(t)\nabla_{\boldsymbol{k}}\rho_{ij}$ in Eq. (1) leads to a fully symmetric distribution of excitation probabilities and also removes the carrier population at $k \gtrsim 0.2k_{max}$.

Interband transitions predominantly occur in the part of the Brillouin zone where the corresponding transition matrix elements $\boldsymbol{d}_{ij}$ have a large magnitude. For transitions from valence bands to the lowest conduction band of GaAs, $|\boldsymbol{d}_{ij}(\boldsymbol{k})|$ are maximal at the Γ point and sharply decrease for $k \gtrsim \Delta k = 0.1k_{max}$ [23, 28]. According to the Bloch acceleration theorem [29], the electron momentum in a given energy band, $\boldsymbol{K}(t)$, changes in time as $\boldsymbol{K}(t) = \boldsymbol{k} - e\hbar^{-1}\int_{t_0}^{t}\boldsymbol{F}(t')dt'$, where $\boldsymbol{k} = \boldsymbol{K}(t_0)$ is the initial momentum. At a characteristic field of $F \sim 0.4$ V/Å, an electron at the Γ point passes through the momentum range of interband transitions during time $\tau \sim \hbar\Delta k/(eF_0) \sim 0.2$ fs. This time interval is much shorter than a half-cycle of both optical oscillations and Rabi oscillations.

Thus we predict a novel regime for solids in strong resonant optical fields where the population oscillations (which become Rabi oscillations in the limit of weaker and longer pulses) are excited by short and strong kicks during times when electrons pass the narrow crystal momentum region Δk near the Γ point. These kicks are repeated twice per optical cycle causing strongly anharmonic (non-sinusoidal in time) Rabi oscillations. We call this regime "*kicked anharmonic Rabi oscillations*" (KARO). It is illustrated in Fig. 4 where we show the time dependence of the lowest CB population for selected reciprocal-space pathways: $n_{c_1}\big(\boldsymbol{K}(t), t\big)$ undergoes very rapid changes at the moments of the kicks, and it is nearly constant between them. Such transitions can excite or de-excite electrons, and their overall outcome depends on the field amplitude and initial momentum $\boldsymbol{k}$, in turn defining whether there is a "bright" (high n_{c_1}) or "dark" (low n_{c_1}) fringe. At the Γ point ($k = 0$) in Fig. 4, the blue curve clearly indicates alternation of such excitation/de-excitation events. For $k \neq 0$ (the green curve), an electron passes near the Γ point at non-equidistant moments of time, which affects the final population and current.

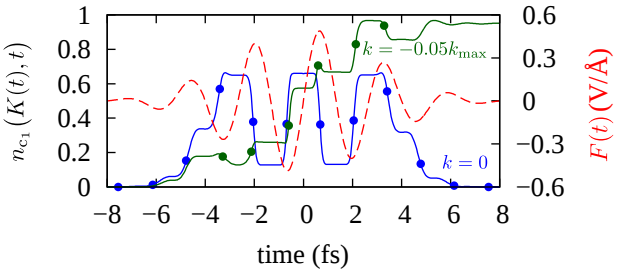

FIG. 4. (Color online) Time dependence of the CB population in the two-band simulation (blue and green curves). It is calculated along reciprocal-space pathways $K(t)$ that satisfy the acceleration theorem. The starting point is the Γ point ($k = 0$) for the blue curve and $k = -0.05k_{\max}$ for the green curve. The bold dots on the curves denote moments of passage in the vicinity of the Γ point. The dashed red curve shows the electric field of the pulse ($F_0 = 0.5$ V/Å, $\varphi_{\rm CE} = \pi/2$).

If the intraband motion is artificially switched off, the fringes in Fig. 3(c) repeat periodically, as expected for Rabi oscillations, and the distribution is precisely symmetric: $n_{c_1}(k, t_{\max}) = n_{c_1}(-k, t_{\max})$. In contrast, the KARO regime in Figs. 3(a) and (b) manifests itself by the fringe spacing increasing with F_0. However, the most important signature of the KARO is the evident asymmetry of the CB density distribution ($k < 0$ vs. $k > 0$), which appears due to the intraband electron motion induced by an ultrashort pulse. The number of Rabi cycles increases with the field amplitude; when the pulse duration corresponds to an integer number of full oscillations, the residual current switches its direction—cf. Fig. 1. We interpret this switching of current as resulting from interference of electron pathways in reciprocal space.

The change of band populations between times t_i and t_f is determined by the field work, $W = \int_{t_i}^{t_f} \boldsymbol{F}(t)\boldsymbol{P}'(t)\,dt$, where $\boldsymbol{P}'(t)$ is the time derivative of the macroscopic polarization induced by both bound and free charges [30]. In the KARO process, the field changes little during a single kick. Consequently, a kick at time t does work $\Delta W \approx \boldsymbol{F}(t)\Delta\boldsymbol{P}(t)$, where $\Delta\boldsymbol{P}$ is the corresponding polarization change. Two kicks that promote electrons from band j to band i at times t_1 and t_2 interfere with each other according to the phase accumulated by the interband polarization between the kicks. For a particular electron with initial crystal momentum $\boldsymbol{k}$, this phase is approximately given by (see Supplemental Material [23])

$$\Delta\phi_{ij}(\boldsymbol{k}) = \frac{1}{\hbar}\int_{t_1}^{t_2} dt\,\Delta E_{ij}\big(\boldsymbol{K}(t)\big). \qquad (3)$$

It is analogous to the Volkov phase [31] in atomic physics. Let us consider two pathways separated by an optical cycle: $t_2 - t_1 = 2\pi/\omega_0$. When $\Delta\phi_{ij}(\boldsymbol{k}) = 2\pi q$, where integer q is the order of a nonlinear resonance, constructive interference results in net excitation of electrons.

In Figs. 3(a)–(b), it is evident that a region of strongly nonlinear behavior occurs at $F_0 \gtrsim 0.5$ V/Å. A nonlinear resonance of the lowest order ($q = 2$) for electron wave packets excited near the Γ point occurs for $\Delta\phi_{ij}(0) = 4\pi$. In a model with two parabolic bands, $\Delta E_{ij}(\boldsymbol{k}) \approx E_g + \hbar^2k^2/(2\mu)$, where μ is reduced effective mass. From Eq. (3), we obtain the second-order resonance condition as $E_g + U_p = 2\hbar\omega_0$, where $U_p = e^2F_0^2/(4\mu\omega_0^2)$ is known as ponderomotive energy. Using $\mu = 0.05m_0$ for transitions from the light-hole VB to the lowest CB in GaAs, we estimate an onset of the resonance at $F_0 = 0.3$ V/Å. A more careful calculation that takes band non-parabolicity into account yields $F_0 = 0.5$ V/Å.

While we have concentrated above on a two-band model, real crystals contain a number of bands that can contribute to nonlinear optical phenomena in strong fields. Figures 3(d)–(f) show that increasing the number of bands to six has a dramatic effect on the simulations for $F_0 \gtrsim 0.1$ V/Å: reciprocal-space populations are perturbed in a highly irregular, quasi-stochastic way; they become significantly asymmetric at lower laser fields, and signatures of Rabi cycles at $\boldsymbol{k} = 0$ are not as clearly visible even if intraband motion is neglected. Apparently, coherent effects suffer from effective dephasing induced by intraband motion in the presence of multiple bands. Similarly to Landau damping [32], this phenomenon is not related to electron-electron collisions or interaction with environment.

Our results also highlight the role of symmetries in strong-field phenomena. For $\varphi_{\rm CE} = 0$, the Hamiltonian is symmetric with respect to time reversal. For $\varphi_{\rm CE} = \pm\pi/2$, it is PT-symmetric, that is, invariant under simultaneous parity (P) and time-reversal (T) transformations. The symmetries of final states match those of the Hamiltonian in two-band simulations (e.g. there is the $\boldsymbol{k} \leftrightarrow -\boldsymbol{k}$ symmetry for $\varphi_{\rm CE} = 0$). Adding more bands breaks this apparent relation (see Figs. 1 and 3).

In conclusion, interaction of strong ultrashort laser pulses with a semiconductor is characterized by rapid passage of the efficient transition region (the vicinity of the Γ point), which brings about a new excitation regime that we call kicked anharmonic Rabi oscillations (KARO). This effect is due to quantum interference between kick-like transitions. Resonances that emerge from interfering kicks manifest themselves in highly asymmetric residual excitation distribution in reciprocal space and, consequently, a strong residual electric current. The predicted effects are experimentally observable: the asymmetric momentum distribution can be directly observed using angular resolved photoemission spectroscopy (ARPES) [33–36], and the residual current can be detected through accompanying terahertz radiation [28, 37, 38]. Our findings add resonant processes to the toolkit of petahertz solid-state technology where potential applications may range from CEP detection [39] to sub-laser-cycle spectroscopy [40] and ultrafast signal processing [6].

We gratefully acknowledge F. Krausz for drawing our interest to resonant strong-field interactions and for his comments. M. S. W. was supported by the International Max Planck Research School of Advanced Photon Science. The work of M. S. W., S. Yu. K. and M. C. was supported by the DFG Cluster of Excellence: Munich-Centre for Advanced Photonics (MAP). The work of M. I. S. was supported by the a MURI Grant #FA9550-15-1-0037 from the US Airforce Office of Scientific Research. A support for V. S. Y. came from a MURI Grant #N00014-13-1-0649 from the US Office of Naval Research.

* michael.wismer@mpq.mpg.de
† stanislav.kruchinin@mpq.mpg.de
‡ mstockman@gsu.edu
§ vyakovlev@gsu.edu

[1] C. Zener, Proc. Royal Soc. London. Ser. A **145**, 523 (1934).
[2] L. V. Keldysh, Sov. Phys. JETP **20**, 1307 (1965).
[3] S. Ghimire, A. D. DiChiara, E. Sistrunk, P. Agostini, L. F. DiMauro, and D. A. Reis, Nature Phys. **7**, 138 (2011).
[4] A. Schiffrin, T. Paasch-Colberg, N. Karpowicz, V. Apalkov, D. Gerster, S. Muehlbrandt, M. Korbman, J. Reichert, M. Schultze, S. Holzner, J. V. Barth, R. Kienberger, R. Ernstorfer, V. S. Yakovlev, M. I. Stockman, and F. Krausz, Nature **493**, 70 (2013).
[5] M. Schultze, E. M. Bothschafter, A. Sommer, S. Holzner, W. Schweinberger, M. Fiess, M. Hofstetter, R. Kienberger, V. Apalkov, V. S. Yakovlev, M. I. Stockman, and F. Krausz, Nature **493**, 75 (2013).
[6] F. Krausz and M. I. Stockman, Nature Photon. **8**, 205 (2014).
[7] M. Schultze, K. Ramasesha, C. D. Pemmaraju, S. A. Sato, D. Whitmore, A. Gandman, J. S. Prell, L. J. Borja, D. Prendergast, K. Yabana, D. M. Neumark, and S. R. Leone, Science **346**, 1348 (2014).
[8] O. Schubert, M. Hohenleutner, F. Langer, B. Urbanek, C. Lange, U. Huttner, D. Golde, T. Meier, M. Kira, S. W. Koch, and R. Huber, Nature Photon. **8**, 119 (2014).
[9] T. T. Luu, M. Garg, S. Yu. Kruchinin, A. Moulet, M. Th. Hassan, and E. Goulielmakis, Nature **521**, 498 (2015).
[10] G. Vampa, T. J. Hammond, N. Thiré, B. E. Schmidt, F. Légaré, C. R. McDonald, T. Brabec, and P. B. Corkum, Nature **522**, 462 (2015).
[11] M. Hohenleutner, F. Langer, O. Schubert, M. Knorr, U. Huttner, S. W. Koch, M. Kira, and R. Huber, Nature **523**, 572 (2015).
[12] G. Vampa, T. J. Hammond, N. Thiré, B. E. Schmidt, F. Légaré, C. R. McDonald, T. Brabec, D. D. Klug, and P. B. Corkum, Phys. Rev. Lett. **115**, 193603 (2015).
[13] D. J. Jones, S. A. Diddams, J. K. Ranka, A. Stentz, R. S. Windeler, J. L. Hall, and S. T. Cundiff, Science **288**, 635 (2000).
[14] S. Hughes, Phys. Rev. Lett. **81**, 3363 (1998).
[15] O. D. Mücke, T. Tritschler, M. Wegener, U. Morgner, and F. X. Kärtner, Phys. Rev. Lett. **87**, 057401 (2001).
[16] O. D. Mücke, T. Tritschler, M. Wegener, U. Morgner, and F. X. Kärtner, Phys. Rev. Lett. **89**, 127401 (2002).
[17] O. D. Mücke, T. Tritschler, M. Wegener, U. Morgner, F. X. Kärtner, G. Khitrova, and H. M. Gibbs, Opt. Lett. **29**, 2160 (2004).
[18] R. Atanasov, A. Haché, J. L. P. Hughes, H. M. van Driel, and J. E. Sipe, Phys. Rev. Lett. **76**, 1703 (1996).
[19] T. M. Fortier, P. A. Roos, D. J. Jones, S. T. Cundiff, R. D. R. Bhat, and J. E. Sipe, Phys. Rev. Lett. **92**, 147403 (2004).
[20] D. Golde, T. Meier, and S. W. Koch, Phys. Rev. B **77**, 075330 (2008).
[21] P. Blaha, K. Schwarz, G. K. H. Madsen, D. Kvasnicka, and J. Luitz, *WIEN2K, An Augmented Plane Wave + Local Orbitals Program for Calculating Crystal Properties* (Karlheinz Schwarz, Techn. Universität Wien, Austria, 2001).
[22] X. Zhang, Y. Jin, and X. F. Ma, Appl. Phys. Lett. **61**, 2764 (1992).
[23] See Supplemental Material at [URL will be inserted by publisher], which includes references [41–49], for details of the model and additional results supporting our main conclusions.
[24] S. S. Prabhu, S. E. Ralph, M. R. Melloch, and E. S. Harmon, Appl. Phys. Lett. **70**, 2419 (1997).
[25] S. Funk, G. Acuna, M. Handloser, and R. Kersting, Opt. Express **17**, 17450 (2009).
[26] P. C. Becker, H. L. Fragnito, C. H. Brito Cruz, R. L. Fork, J. E. Cunningham, J. E. Henry, and C. V. Shank, Phys. Rev. Lett. **61**, 1647 (1988).
[27] Q. T. Vu, H. Haug, O. D. Mücke, T. Tritschler, M. Wegener, G. Khitrova, and H. M. Gibbs, Phys. Rev. Lett. **92**, 217403 (2004).
[28] W. Kuehn, P. Gaal, K. Reimann, M. Woerner, T. Elsaesser, and R. Hey, Phys. Rev. B **82**, 075204 (2010).
[29] F. Bloch, Z. Phys. A **52**, 555 (1929).
[30] L. D. Landau and E. M. Lifshitz, *Electrodynamics of Continuous Media* (Pergamon, Oxford and New York, 1984).
[31] D. Wolkow, Zeitschrift für Physik **94**, 250 (1935).
[32] L. D. Landau, Journal of Physics **10**, 25 (1946).
[33] A. Damascelli, Z. Hussain, and Z. X. Shen, Rev. Mod. Phys. **75**, 473 (2003).
[34] S. Mathias, L. Miaja-Avila, M. M. Murnane, H. Kapteyn, M. Aeschlimann, and M. Bauer, Rev. Sci. Instrum. **78**, 083105 (2007).
[35] J. Güdde, M. Rohleder, T. Meier, S. W. Koch, and U. Höfer, Science **318**, 1287 (2007).
[36] W. S. Lee, I. M. Vishik, D. H. Lu, and Z. X. Shen, J. Phys.: Condensed Matter **21**, 164217 (2009).
[37] D. Côté, J. M. Fraser, M. DeCamp, P. H. Bucksbaum, and H. M. van Driel, Appl. Phys. Lett. **75**, 3959 (1999).
[38] M. Spasenović, M. Betz, L. Costa, and H. M. van Driel, Phys. Rev. B **77**, 085201 (2008).
[39] T. Paasch-Colberg, A. Schiffrin, N. Karpowicz, S. Kruchinin, Ö. Sağlam, S. Keiber, O. Razskazovskaya, S. Mühlbrandt, A. Alnaser, M. Kübel, V. Apalkov, D. Gerster, J. Reichert, T. Wittmann, J. V. Barth, M. I. Stockman, R. Ernstorfer, V. S. Yakovlev, R. Kienberger, and F. Krausz, Nature Photon. **8**, 214 (2014).
[40] M. Ivanov and O. Smirnova, Chem. Phys. **414**, 3 (2013).
[41] F. Tran and P. Blaha, Phys. Rev. Lett. **102**, 226401 (2009).
[42] J. Blakemore, J. Appl. Phys. **53**, R123 (1982).
[43] Y. A. Bychkov and A. M. Dykhne, Sov. Phys. JETP **31**, 928 (1970).

[44] J. B. Krieger and G. J. Iafrate, Phys. Rev. B **33**, 5494 (1986).
[45] S. Yu. Kruchinin, M. Korbman, and V. S. Yakovlev, Phys. Rev. B **87**, 115201 (2013).
[46] L. Huang, J. P. Callan, E. N. Glezer, and E. Mazur, Phys. Rev. Lett. **80**, 185 (1998).
[47] L. Hedin, Phys. Rev. **139**, A796 (1965).
[48] M. S. Hybertsen and S. G. Louie, Phys. Rev. B **34**, 5390 (1986).
[49] F. Aryasetiawan and O. Gunnarsson, Rep. Progr. Phys. **61**, 237 (1998).